DFT CALCULATION AND RAMAN SPECTROSCOPY STUDIES OF α-LINOLENIC ACID

Heng Peng[a], Hua-Yi Hou[a] and Xiang-Bai Chen[a],*, [ORCID]

[a]Hubei Key Laboratory of Optical Information and Pattern Recognition, Wuhan Institute of Technology, Wuhan 430205, China

Density functional theory (DFT) calculation and Raman scattering experiment have been applied to investigate an important essential fatty acid, α-linolenic acid (ALA). The DFT calculation was performed with geometry optimization and harmonic vibration using B3LYP functions with polarized 6-311+G(d,p) basis. The DFT calculated vibrational modes of ALA molecule are in excellent agreement with the Raman experimental results. A complete vibrational modes assignment is provided on the basis of potential energy distribution calculation. In addition, the DFT calculation and Raman experiment indicate that the relative intensity ratio of two characteristic modes at 1660 cm^{-1} and 1440 cm^{-1} is correlated with the number of C=C double bond in the acid chain, which may provide a simple and convenient method to differentiate ALA with other types of unsaturated fatty acids. Furthermore, the Mulliken atomic charge distribution and frontier molecular orbitals of ALA molecule were calculated.

Keywords: α-Linolenic acid; DFT calculation; Raman spectroscopy; atomic charge distribution; frontier molecular orbital.

INTRODUCTION

α-Linolenic acid (ALA), an important essential fatty acid (EFA), has 18 carbons in the acid chain with three *cis* double bonds. ALA is described as an n-3 polyunsaturated fatty acid (PUFA), its first double bond is located on the third carbon from its methyl terminal, and the other two double bonds are located on the sixth and ninth carbon respectively. For mammals, ALA cannot be synthesized directly, it must be provided through dietary intake.[1] ALA can be found in seeds, nuts, and many leafy vegetable oils, especially in flaxseed with high content.[2] It has been reported that ALA shows positive effects for chronic diseases including cancer, insulin resistance, and cardiovascular.[3-5] An important role of ALA is assumed to be a precursor to the longer chain eicosapentaenoic acid (EPA) and docosahexanoic acid (DHA), which play a vital role in brain development.[6] The metabolic pathway of ALA to EPA and DHA involves complex steps.[7] The study of molecular vibrational properties of ALA will be useful for differentiating ALA with other unsaturated fatty acids and understanding the metabolic pathway of ALA.

Raman spectroscopy, a powerful fast and non-destructive analytical technique, has been widely used for research in many varied fields.[8-11] It can provide information about molecular vibrations that can be used for sample identification. However, only through Raman spectroscopy experiment is difficult to have a good understanding of molecular vibrational properties, especially for large molecules. Theoretical calculation and comparison of theoretical and experimental results are necessary for a systematic study of molecular vibrational property. It has been shown that density functional theory (DFT) calculation can provide reliable and accurate results for predicting and assigning vibrational modes of various molecules.[12-17] Raman spectroscopy and DFT calculation have been applied to study oleic acid and linoleic acid, which have one and two C=C double bonds, respectively.[18,19] In the present work, we apply Raman scattering experiment and DFT calculation to investigate the molecular vibrational properties of ALA, which has three C=C double bonds. Excellent agreement between DFT calculation and Raman experiment were achieved with very good linear relation of R^2 (0.99978) and very small deviations (less than

10 cm^{-1}). The vibrational modes assignments were interpreted with a high degree of accuracy on the basis of potential energy distributions (PED) calculation using the VEDA 4.0 program.[20,21] In addition, the Mulliken atomic charge distribution and frontier molecular orbitals of ALA molecule were calculated.

EXPERIMENTAL

The ALA sample was purchased from MOLBASE with a stated purity greater than 97% and used as received. Raman scattering experiments of ALA sample were performed in backscattering configuration with a Thermo Fisher DXR micro-Raman spectrometer and a Nanobase XperRam micro-Raman spectrometer. In both systems, excitation laser of 532 nm was applied; the scattered signal was detected by an air-cooled CCD detector. The spectra were corrected in wavenumber by using the 521 cm^{-1} vibrational mode of a Si substrate.

For the DFT calculation, we employed the commonly applied method of Becke's 1988 exchange functional in combination with Becke's three-parameter hybrid exchange functional using the LYP correlation functional of Lee, Yang, and Parr (B3LYP).[22-25] For geometry optimization and analytical vibration frequency calculation, the polarized 6-311+G(d,p) basis was applied with d polarization functions on heavy atoms and p polarization functions on hydrogen atoms as well as diffuse functions for heavy atoms. The quantum mechanical calculations were performed using the Gaussian09 program.[26] The vibrational wavenumbers were assigned on the basis of potential energy distribution calculation using VEDA 4.0 program.[20,21] Calculated data analyzing and graph plotting were performed using the Multiwfn_3.4.1(dev) program.[27] Lorentzian curve has been chosen for the line shape and 4 cm^{-1} has been chosen for the full width at half maximum of each peak. The Mulliken atomic charge distribution and frontier molecular orbitals were calculated with the same DFT method.

RESULTS AND DISCUSSION

Figure 1 presents the experimental and calculated Raman spectra of ALA molecule. The experimental spectrum recorded in the spectral range of 100-3500 cm^{-1} was from a Thermo Fisher DXR micro-Raman

*e-mail: xchen@wit.edu.cn

system. The inset spectrum zoomed in the spectral range of 100-1000 cm^{-1} was from a Nanobase XperRam micro-Raman system. ALA has the molecular formula of $C_{18}H_{30}O_2$ with molecular structure as shown in the insert of Figure 1. The vibrational modes of ALA molecule are both infrared and Raman active, which is due to the C1 point group symmetry. In Figure 1, 74 vibrational modes were experimentally observed in the spectral range of 100-3500 cm^{-1}. For the assignment of these vibrational modes, DFT calculation was performed, the calculated spectrum is also presented in Figure 1.
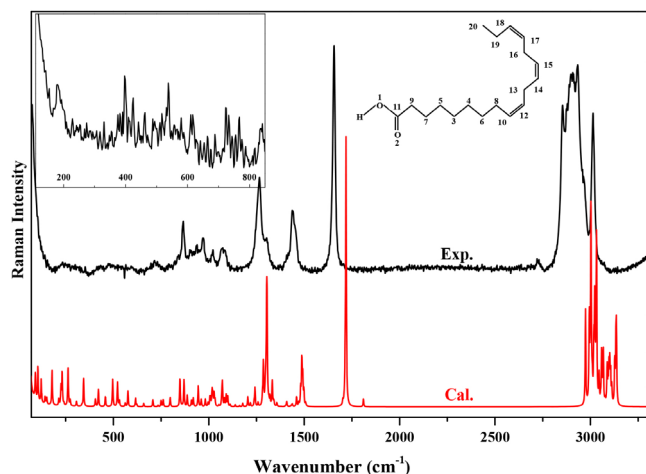
Figure 1. *Experimental and calculated Raman spectra of ALA, the ALA molecular structure is shown in the insert*

In the DFT calculation, the ground-state geometry of ALA molecule was optimized at B3LYP/6-311+G(d,p) level of theory without any symmetry restrain for achieving accurate analytical vibrational frequency calculation. The optimized structure was confirmed to be minimum energy conformation. The calculated result showed that there is no imaginary frequency at the optimized structure of the ALA molecule. Therefore a true minimum on the potential energy surface was found for the ALA molecule. The calculated bond lengths and bond angles of ALA molecule are presented in Table 1.

Table 1. Calculated bond lengths and bond angles of ALA molecule

Bond	Cal. length (Å)	Bond	Cal. angle (°)
O1-C11	1.3588	C4-C3-C5	113.4897
O1-H	0.9692	C3-C4-C6	113.2847
O2=C11	1.2057	C3-C5-C7	113.0784
C3-C4	1.5328	C4-C6-C8	114.0404
C3-C5	1.5328	C5-C7-C9	113.7715
C4-C6	1.5325	C6-C8-C10	113.2579
C5-C7	1.5335	C7-C9-C11	114.0322
C6-C8	1.5418	O1-C11-O2	122.0911
C7-C9	1.5309	O1-C11-C9	111.4637
C8-C10	1.505	O2-C11-C9	126.4283
C9-C11	1.5118	C10=C12-13	128.0164
C10=C12	1.3356	C4-C3-C5	113.4897
C12-C13	1.5102	C3-C4-C6	113.2847
C13-C14	1.5099	C12-C13-C14	112.0295
C14=C15	1.3356	C13-C14=C15	128.0647
C15-C16	1.5105	C14=C15-C16	128.0182
C16-C17	1.511	C15-C16-C17	111.7379
C17=C18	1.3365	C16-C17=C18	127.9366
C18-C19	1.5043	C17=C18-C19	128.4104
C19-C20	1.5382	C18-C19-C20	112.5096

For further agreement between calculated wavenumbers with experimental results, i.e., to obtain small derivations and good linear correlation between calculated and experimental results, the calculated wavenumbers are normally scaled with a necessary wavenumber linear scaling (WLS) procedure by accounting anharmonicity in DFT calculation.[28] In this study, the calculated wavenumbers of all the vibrational modes in the whole spectral range of 100-3500 cm^{-1} have been scaled down by the equation: $v_{obs}/v_{cal} = 1.0087 - 0.0000163 v_{cal}$.[28] The correlation of experimental and calculated wavenumbers is plotted in Figure 2, and fitted with a linear line. Our results show that the deviations are less than 10 cm^{-1} between calculated and experimental wavenumbers. All the modes provide a very good linear correlation between calculated and experimental wavenumbers with R^2 of 0.99978. The vibrational modes assignments have been performed based on the comparison of experimentally observed Raman peaks with DFT calculated wavenumbers, the results are presented in Table 2.

The number of C=C double bonds in the acid chain is the major difference of ALA comparing with other types of unsaturated fatty acids, such as longer chain acids of EPA and DHA correlated with the metabolic pathway, oleic acid (most common monounsaturated fatty acid), linoleic acid (another well known essential fatty acid having two C=C double bonds), etc. In Figure 1, the Raman vibrational modes at 1660 and 1440 cm^{-1} have strong intensity and are weakly affected by their neighboring vibrational modes. The mode at 1660 cm^{-1} is correlated with the vibration of C=C double bond, and the mode at 1440 cm^{-1} is correlated with the vibration of C-H bond. ALA molecule has three C=C double bonds, interestingly the relative intensity ratio of 1660 and 1440 cm^{-1} is also about 3. In addition, in a previous study of Raman spectra of oleic acid (one C=C double bond) and linoleic acid (two C=C double bonds), it was indicated that the relative intensity ratio of 1660 and 1440 cm^{-1} was about 1 and 2, respectively.[29] Therefore, fully understanding the relative intensity ratios of characteristic vibrational modes in unsaturated fatty acids would be interesting, it may provide a simple and convenient method to differentiate different types of unsaturated fatty acids. A systematic study of the correlation of relative intensity ratios with C=C double bonds in various different types of unsaturated fatty acids up to six C=C double bonds is currently underway and will be presented elsewhere.

In our DFT calculation, the analyses of Mulliken atomic charge distribution and frontier molecular orbitals of ALA molecule were also performed. The Mulliken atomic charge distribution of a molecule has significant influence on dipole moment, polarizability, electronic structure and vibrational modes.[30] In the present work, the Mulliken atomic charge distribution was predicted for the ALA molecule by using the DFT/B3LYP method. The calculated Mulliken atomic charge values are presented in Table 3, and the Mulliken atomic charge distribution is plotted in Figure 3. The Mulliken atomic charge distribution has been used to describe the process of electronegativity equalization and model of electrostatic potential outside the molecular surface.[30] In the molecular of ALA, all H atoms have a positive charge, the C atoms (except C4 and C5) and O atoms have negative charges.

The highest occupied molecular orbital (HOMO) and lowest unoccupied molecular orbital (LUMO) are referred as "frontier orbitals", which act as the essential part in a wide range of chemical reactions. The HOMO energy characterizes the ability of electron giving, the LUMO energy characterizes the ability of electron accepting, and the gap between HOMO and LUMO characterizes the molecular chemical stability and electron conductivity.[31,32] In the present work, the frontier molecular orbitals analysis of ALA was performed using the DFT/B3LYP method. The calculated frontier orbitals HOMO and LUMO of ALA molecule are presented in Figure

Table 2. Experimental, calculated, and assignment of vibrational modes of ALA molecule

Exp.	Cal.		Assignment(%PED)
	Scaled	Unscaled	
	92	91	τ(C11C9C7C5)(20)+τ(C4C6C8C10)(25)+τ(C9C7C5C3)(14)
	105	104	β(C3C4C6)(18)+β(C5C3C4)(16)+β(C7C5C3)(13)+τ(C11C9C7C5)(17)
	123	122	τ(C5C3C4C6)(18)
142v	143	142	β(C17C16C15)(16)+τ(C7C5C3C4)(15)
154vw	151	150	τ(C4C6C8C10)(12)+τ(C5C3C4C6)(26)+τ(C7C5C3C4)(11)
182vw	179	178	β(C15=C14C13)(11)+β(C18=C17C11)(16)+β(C19C18=C17)(16)+β(C16C15=C14)(17)
	215	214	β(C12=C10C8)(15)+β(C13C12=C10)(12)+β(C4C6C8)(11)+β(C7C5C3)(10)
228vw	226	225	β(C14C13C12)(19)+β(C20C19C18)(14)+τ(C19C18=C17C16)(13)
	232	231	β(C11C9C7)(18)+β(C9C7C5)(15)
	241	240	τ(H₃C20C19C18)(49)
	263.	262	β(C12=C10C8)(14)+β(C13C12=C10)(17)+β(C4C6C8)(10)
274vw	275	274	β(O1C11C9)(21)+β(C11C9C7)(18)+β(C3C4C6)(12)
	307	306	β(C6C8C10)(13)+β(C20C19C18)(12)+τ(C13C12=C10C8)(10)
330vw	336	335	β(C15=C14C13)(19)+β(C18=C17C16)(18)+β(C19C18=C17)(16)+β(C16C15=C14)(12)
	345	344	β(C14C13C12)(13)+β(C17C16C15)(14)+β(C6C8C10)(11)+β(C20C19C18)(16)
396w	407	406	β(O1C11C9)(12)+β(C3C4C6)(10)+β(C5C3C4)(26)+β(C9C7C5)(15)
424vw	423	422	β(C4C6C8)(14)+τ(C13C12=C10C8)(12)
462vw	459	458	β(C20C19C18)(10)+τ(C16C15=C14C13)(17)
494vw	496	496	β(C12=C10C8)(11)+τ(C13C12=C10C8)(12)
517vw	521	521	τ(HO1C11C9)(11)+τ(C19C18=C17C16)(11)
	522	522	τ(HO1C11C9)(27)+o(O2C9O1C11)(20)
538w	532	532	β(O2=C11O1)(17)+β(O1C11C9)(16)+β(C7C5C3)(11)
	562	562	β(C18=C17C16)(21)+β(C19C18=C17)(19)
577vw	576	576	β(C15=C14C13)(13)+β(C16C15=C14)(13)
611vw	615	616	β(O2=C11O1)(18)+β(C12=C10C8)(11)+β(C13C12=C10)(12)
618vw	622	623	β(O2C11=O1)(27)
	658	659	τ(HO1C11C9)(11)+o(O2C9O1C11)(30)
	705	707	τ(HC10=C12C13)(29)+τ(HC12=C10C8)(31)
723vw	731	733	τ(HC3C5C7)(11)+τ(HC14=C15C16)(13)+τ(HC15=C14C13)(12)
733vw	733	735	τ(HC14=C15C16)(17)+τ(HC15=C14C13)(16)
	747	750	τ(HC4C6C8)(13)
767vw	758	761	τ(HC14=C15C16)(10)+τ(HC17=C18C19)(22)+τ(HC18=C17C16)(23)
	794	797	τ(HC20C19C18)(12)
	795	798	ν(C11C9)(10)+τ(HC20C19C18)(12)
845vw	845	849	ν(C11C9)(22)
851vw	855	860	ν(C4C6)(15)+ν(C7C5)(10)+τ(HC8C10=C12)(12)
866m	865	870	ν(C11C9)(31)+ν(C20C19)(14)+τ(HC20C19C18)(10)
879w	882	887	ν(C7C5)(11)+τ(HC9C11O1)(17)+ o(O2C9O1C11)(14)
903w	903	909	ν(C16C15)(14)+τ(HC16C17=C18)(14)
910w	913	919	ν(C16C15)(11)
942w	938	944	ν(C14C13)(14)+ν(C17C16)(10)
953w	953	960	ν(C16C15)(18)+τ(HC13C12=C10)(13)
975m	975	982	skeletal twisting
996	998	1006	ν(C14C13)(12)+ν(C20C19)(17)

Table 2. Experimental, calculated, and assignment of vibrational modes of ALA molecule (cont.)

Exp.	Cal.		Assignment(%PED)
	Scaled	Unscaled	
1000vw	1001	1009	τ(HC10=C12C13)(15)+τ(HC12=C10C8)(22)
1006w	1008	1016	τ(HC15=C14C13)(11)
	1010	1018	τ(HC14=C15C16)(14)+τ(HC17=C18C19)(24)+τ(HC18=C17C16)(19)+τ(C19C18=C17C16)(12)
1014	1013	1021	τ(HC14=C15C16)(10)+τ(HC15=C14C13)(10)
	1020	1028	ν(C19C18)(10)+ν(C17C16)(13)+ν(C20C19)(28)
1024m	1025	1033	ν(C13C12)(13)
1041vw	1044	1053	ν(C3C4)(21)+ν(C5C3)(30)
1058vw	1057	1068	ν(C3C4)(14)+ν(C4C6)(14)+ν(C9C7)(12)+ν(C6C8)(16)
1069m	1062	1071	ν(C4C6)(13)+ν(C5C3)(13)+ν(C7C5)(18)
1076m	1072	1082	ν(C16C15)(10)+ν(C7C5)(11)
1082m	1081	1091	τ(HC19C18=C17)(16)+τ(HC20C19C18)(24)
1088m	1090	1100	ν(C4C6)(11)
1107w	1102	1112	ν(O1C11)(27)+β(HO1C11)(11)+β(HC7C9)(12)
1130w	1128	1139	τ(HC20C19C18)(10)
1152vw	1149	1161	skeletal twisting
1159w	1166	1178	ν(O1C11)(13)+β(HC7C9)(14)
1189vw	1191	1204	β(HC8C10)(13)+β(HC9C11)(13)
1202vw	1204	1218	β(HC13C14)(18)+β(HC16C17)(13)
1219vw	1224	1238	β(HC13C14)(18)+β(HC16C17)(21)+τ(HC16C17=C18)(11)
	1228	1242	β(HC8C10)(18)+β(HC9C11)(21)
1241m	1243	1258	τ(HC3C5C7)(12)+τ(HC5C7C9)(11)
1266vs	1265	1281	β(HC18C19)(13)+β(HC19C20)(20)+τ(HC19C18=C17)(12)
	1270	1286	skeletal twisting
	1271	1287	β(HC8C10)(12)+τ(HC3C5C7)(10)
	1279	1295	β(HC15C16)(13)+β(HC17=C18)(11)+β(HC19C20)(16)+τ(HC16C17=C18)(12)
	1282	1298	β(HO1C11)(20)+β(HC10=C12)(10)
1284s	1287	1303	β(HC18C19)(14)+β(HC16C17)(11)
	1289	1305	β(HC18C19)(14)+β(HC16C17)(11)
1298s	1297	1314	τ(HC16C17=C18)(12)
1303s	1303	1320	Skeletal vibration -(CH2)7- in phase twisting
	1315	1332	β(HC3C5)(14)+β(HC4C6)(27)+τ(HC6C8C10)(12)
	1316	1333	β(HC3C5)(26)+β(HC5C7)(18)+τ(HC4C6C8)(14)
1321w	1322	1340	β(HC4C6)(10)+β(HC5C7)(19)+β(HC7C9)(13)+τ(HC5C7C9)(12)
	1324	1342	τ(H₂C19C18=C17)(45)
1337w	1339	1357	β(HC6C8)(21)+τ(H₂C8C10C12)(25)
	1359	1378	τ(H₂C3C5C7)(21)+τ(H₂C6C8C10)(28)+τ(H₂C7C9C11)(21)
	1381	1401	τ(H₂C4C6C8)(34)
	1386	1406	τ(H₂C5C7C9)(35)+τ(H₂C7C9C11)(22)
1378vw	1388	1408	ν(C11C9)(11)+β(HC7C9)(11)+β(HC9C11)(12)+τ(HC9C11O1)(19)
	1389	1409	β(C20H₃)(85)
	1407	1428	β(HC14=C15)(35)+β(HC15C16)(32)
	1414	1435	β(HC17=C18)(33)+β(HC18C19)(29)
1416w	1417	1438	β(HC10C12)(35)+β(HC12C13)(34)
1442s	1438	1460	β(C9H₂)(81)

Table 2. Experimental, calculated, and assignment of vibrational modes of ALA molecule (cont.)

Exp.	Cal.		Assignment(%PED)
	Scaled	Unscaled	
1450s	1449	1471	$\beta(C8H_2)(11)+\beta(C13H_2)(55)+\beta(C16H_2)(21)$
1457s	1458	1481	$\beta(C8H_2)(18)+\beta(C18H_2)(41)+\beta(C19H_2)(20)$
	1459	1482	$\beta(C5H_2)(17)+\beta(C7H_2)(65)$
	1463	1486	$\beta(C3H_2)(17)+\beta(C6H_2)(39)$
	1465	1488	$\beta(C8H_2)(41)+\beta(C13H_2)(12)+\beta(C19H_2)(10)$
	1466	1489	$\beta(C8H_2)(41)+\beta(C13H_2)(12)+\beta(C19H_2)(10)$
	1469	1492	$\beta(C16H_2)(21)+\beta(C19H_2)(27)+\beta(C20H_2)(15)$
1473w	1474	1498	$\beta(C20H_3)(75)+\tau(HC20C19C18)(15)$
1484w	1483	1507	$\beta(C19H_2)(22)+\beta(C20H_3)(48)$
1494vw	1487	1511	$\beta(C3H_2)(32)+\beta(C4H_2)(31)+\beta(C5H_2)(19)$
1660vs	1670	1702	$\nu(C15=C14)(36)+\nu(C18=C17)(36)$
	1682	1715	$\nu(C12=C10)(52)+\nu(C18=C17)(15)$
	1686	1719	$\nu(C12=C10)(20)+\nu(C15=C14)(32)+\nu(C18=C17)(22)$
	1772	1810	$\nu(O2=C11)(85)$
2855vs	2856	2974	$\nu(C13H)(98)$
	2873	2993	$\nu(C3H_2)(77)$
	2874	2994	$\nu(C4H)(21)+\nu(C6H_2)(31)+\nu(C8H)(34)$
2877vs	2878	2998	$\nu(C4H)(19)+\nu(C5H)(49)+\nu(C8H)(18)$
2883vs	2882	3003	$\nu(C19H)(93)$
2887vs	2889	3010	$\nu(C4H)(27)+\nu(C6H_2)(37)$
	2896	3018	$\nu(C3H_2)(56)+\nu(C4H)(21)+\nu(C5H)(11)$
2898vs	2899	3022	$\nu(C7H)(45)+\nu(C9H)(27)$
2900vs	2900	3023	$\nu s(C20H_3)(100)$
	2906	3029	$\nu(C4H)(14)+\nu(C6H_2)(57)$
2908vs	2908	3031	$\nu(C16H_2)(95)$
	2909	3032	$\nu(C7H_2)(33)+\nu(C9H_2)(59)$
	2920	3045	$\nu(C4H)(12)+\nu(C5H)(45)+\nu(C6H)(10)+\nu(C7H)(16)$
2925vs	2928	3053	$\nu(C4H)(19)+\nu(C7H)(11)+\nu(C8H)(30)$
	2933	3059	$\nu(C16H_2)(40)+\nu(C19H)(41)$
2935vs	2934	3060	$\nu(C8H)(48)$
	2939	3065	$\nu(C5H)(13)+\nu(C9H_2)(55)$
	2941	3068	$\nu(C16H_2)(44)+\nu(C19H)(28)$
	2949	3077	$\nu(C7H_2)(52)+\nu(C9H)(32)$
2959s	2959	3087	$\nu(C19H)(13)+\nu(C20H)(93)$
2965s	2963	3092	$\nu a(C20H_3)(90)$
2968s	2968	3097	$\nu(C10H)(18)+\nu(C12H)(20)+\nu(C13H)(50)$
	2972	3102	$\nu(C10H)(46)+\nu(C12H)(13)+\nu(C13H)(24)+\nu(C14H)(13)$
	2978	3106	$\nu(C17H)(24)+\nu(C18H)(69)$
	2981	3112	$\nu(C13H)(13)+\nu(C14H)(47)+\nu(C15H)(30)$
	2995	3127	$\nu(C10H)(24)+\nu(C12H)(62)$
3014vs	3000	3133	$\nu(C17H)(74)+\nu(C18H)(24)$
	3003	3136	$\nu(C14H)(35)+\nu(C15H)(57)$
	3559	3756	$\nu(O1H)(100)$

Note: Assignments and potential energy distribution (PED) (contribution≥10%) for vibrational normal modes. Types of vibration: ν=stretching; τ=torsion; νa=asymmetrical stretching; β=bending; o=out of plane bending. All the wavenumbers are in cm^{-1}.
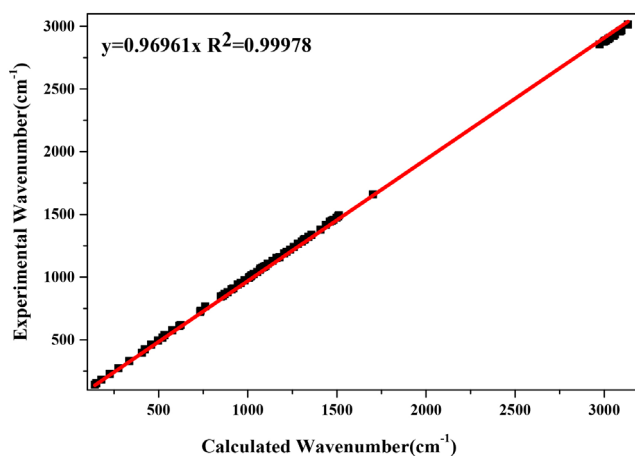
Figure 2. The linear fitting of calculated and experimental wavenumbers
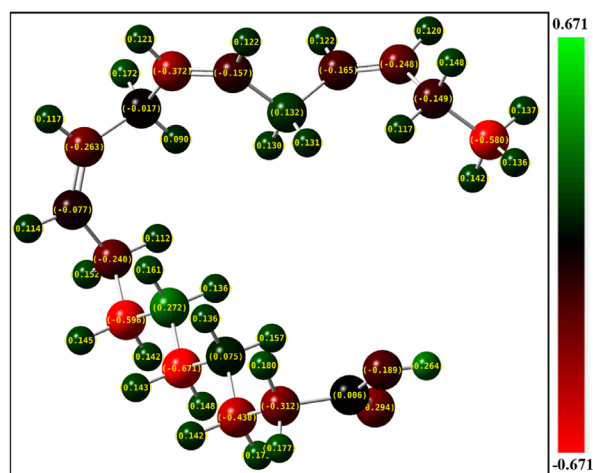

Figure 3. The Mulliken atomic charge distribution of ALA molecule

Table 3. Calculated Mulliken atomic charge distribution of ALA molecule

| Atom. No	Atom	Charge value	Atom. No	Atom	Charge value
1	O	-0.092629	26	H	0.163846
2	O	-0.247065	27	H	0.147823
3	C	-1.024457	28	H	0.148889
4	C	0.531538	29	H	0.180420
5	C	0.408055	30	H	0.148503
6	C	-0.745203	31	H	0.150366
7	C	-0.489390	32	H	0.124910
8	C	-0.285638	33	H	0.173569
9	C	-0.320733	34	H	0.183291
10	C	-0.012076	35	H	0.115571
11	C	-0.214537	36	H	0.127846
12	C	-0.324474	37	H	0.122075
13	C	-0.133935	38	H	0.160727
14	C	-0.277082	39	H	0.124666
15	C	-0.440511	40	H	0.118567
16	C	0.324494	41	H	0.139245
17	C	-0.135037	42	H	0.158644
18	C	-0.236665	43	H	0.262171
19	C	-0.213247	44	H	0.116242
20	C	-0.483264	45	H	0.124706
21	H	0.146325	46	H	0.138516
22	H	0.150320	47	H	0.138268
23	H	0.166686	48	H	0.149711
24	H	0.139461	49	H	0.135472
25	H	0.147853	50	H	0.107167
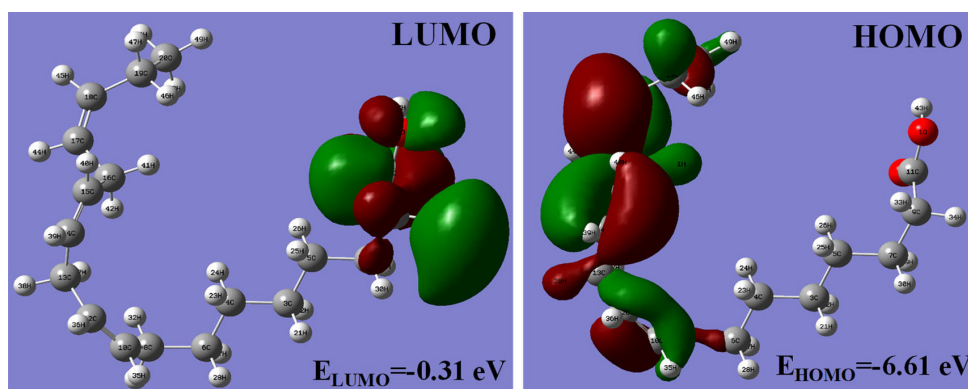
Figure 4. The HOMO and LUMO orbitals of ALA molecule

4, which shows that the energy gap between HOMO and LUMO is about 6.30 eV. The calculated energy gap indicates that the ALA molecule has a stable structure. The HOMO-LUMO transition is correlated with a redistribution of electronic charge between methyl group and carboxyl group.

CONCLUSIONS

The vibrational properties of ALA have been investigated by DFT calculation and Raman spectroscopy experiment. The DFT calculated spectrum of ALA is in excellent agreement with the Raman experimental spectrum. The deviations of calculated and experimental wavenumbers are smaller than 10 cm^{-1} and there is a very good linear relation with R^2 of 0.99978. Also, the calculated bond lengths and bond angles of ALA molecule were listed for further study. In addition, the Mulliken atomic charge distribution and frontier molecular orbitals were calculated.

ACKNOWLEDGEMENTS

REFERENCES

1. Sinclair, A. J.; Attar-Bashi, N. M.; Lib, D.; *Lipids* **2002**, *37*, 1113.
2. Raper, N. R.; Cronin, F. J.; Exler, J.; *J. Am. Coll. Nutr.* **1992**, *11*, 304.
3. Stéfani, E. D.; Deneo-Pellegrini, H.; Boffetta, P.; Ronco, A.; Mendilaharsu, M.; *Cancer Epidemiol. Biomarkers Prev.* **2000**, *9*, 335.
4. Enriquez, Y. R.; Giri, M.; Rottiers, R.; Christophe, A.; *Clin. Chim. Acta* **2004**, *346*, 145.
5. Wendland, E.; Farmer, A.; Glasziou, P.; Neil, A.; *Heart* **2006**, *92*, 166.
6. Crawford, M. A.; Sinclair, A. J.; *Ciba Found. Symp.* **1971**, 267.
7. Fekete, K.; Decsi, T.; *Nutrients* **2010**, *2*, 965.
8. Chen, X. B.; Kong, M. H.; Choi, J. Y.; Kim, H. T.; *J. Phys. D. Appl. Phys.* **2016**, *49*, 465304.
9. Chen, X. B.; Guo, P. C.; Huyen, N. T.; Kim, S.; Yang, I. S.; Wang, X.; Cheong, S. W.; *Appl. Phys. Lett.* **2017**, *110*, 122405.
10. Hou, H. Y.; Yang, X.; Mao, Z. L.; Yao, X. Y.; Chen, X. B.; *Spectrochim. Acta A* **2019**, *221*, 117206.
11. Peng, H; Wu, D.X.; Hou, H. Y.; Chen, X. B.; *J. Appl. Spectrosc.* **2020**, *87*, 548.
12. Paczkowska, M.; Mizera, M.; Dzitko, J.; Lewandowska, K.; Zalewski, P.; Cielecka-Piontek, J.; *J. Mol. Struct.* **2017**, *1134*, 135.
13. Zhou, S.; You, B.; Yao, Q.; Chen, M.; Wang, Y.; Li, W.; *Spectrochim. Acta A* **2013**, *110*, 333.
14. Mariappan, G.; Sundaraganesan, N.; Manoharan, S.; *Spectrochim. Acta A* **2012**, *95*, 86.
15. Rossi, B.; Verrocchio, P.; Viliani, G.; Mancini, I.; Guella, G.; Rigo, E.; Scarduelli, G.; Mariotto, G.; *J. Raman Spectrosc.* **2009**, *40*, 453.
16. Keresztury, G.; Holly, S.; Besenyei, G.; Varga, J.; Wang, A.; Durig, J. R.; *Spectrochim. Acta A* **1993**, *49*, 2019.
17. Contreras, C. D.; Ledesma, A. E.; Zinczuk, J.; Brandán, S. A.; *Spectrochim. Acta A* **2011**, *79*, 1710.
18. Mishra, S.; Chaturvedi, D.; Kumar, N.; Tandon, P.; Siesler, H. W.; *Chem. Phys. Lipids* **2010**, *163*, 207.
19. Machado, N. F. L.; Batista de Carvalho, L. A. E.; Otero, J. C.; Marques, M. P. M.; *J. Raman Spectrosc.* **2012**, *43*, 1991.
20. Jamróz, M. H.; *Vibrational Energy Distribution Analysis*: VEDA 4, program, Warsaw, 2004–2010.
21. Jamróz, M. H.; *Spectrochim. Acta A* **2013**, *114*, 220.
22. Becke, A. D.; *J. Chem. Phys.* **1996**, *104*, 1040.
23. Becke, A. D.; *Phys. Rev. A* **1998**, *38*, 3098.
24. Becke, A. D.; *J. Chem. Phys.* **1993**, 98, 1372.
25. Lee, C.; Yang, W.; Parr, R. G.; *Phys. Rev. B* **1988**, *37*, 785.
26. Kuno, M.; Caricato, M.; Frisch, M. J.; Hiscocks, J.; Barone, V.; Bloino, J.; Biczysko, M.; *MRS Bull.* **2013**, *37*, 1.
27. Lu, T.; Chen, F.; *J. Comput. Chem.* **2012**, *33*, 580.
28. Yoshida, H.; Takeda, K.; Okamura, J.; Ehara, A.; Matsuura, H.; *J. Phys. Chem. A* **2002**, *106*, 3580.
29. Fan, Y.; Li, S.; Xu, D.; *Spectrosc. Spect. Anal.* **2013**, *33*, 3240.
30. Premkumar, S.; Jawahar, A.; Mathavan, T.; Kumara Dhas, M.; Sathe, V. G.; Benial, A. M. F.; *Spectrochim. Acta A* **2014**, *129*, 74.
31. Fukui, K.; *Angew. Chem., Int. Ed.* **1982**, *21*, 801.
32. Karabacak, M.; Cinar, M.; Kurt, M.; *Spectrochim. Acta A* **2009**, *74*, 1197.